POAC'13
Espoo, Finland

Proceedings of the 22nd International Conference on
Port and Ocean Engineering under Arctic Conditions
June 9-13, 2013
Espoo, Finland

ON THE RESULTS OF RESEARCH OF THE INTERNAL STRUCTURE OF ICE RIDGES IN THE "NORTH POLE – 2010" EXPEDITION AT BARNEO ICE CAMP IN APRIL 2010

Victor V. Kharitonov
Arctic and Antarctic Research Institute, St. Petersburg, Russia

ABSTRACT

Arctic and Antarctic Research Institute (AARI) continues studying the morphometric characteristics of ice ridges in the central part of Arctic basin. This paper is aimed to present the information about internal structure of ice ridges studied during April 2010 near Barneo ice camp. Methods and results of studying of several ice ridges of different morphology are discussed. Maximum keel draft and sail height were within the intervals from 7.3 to 12 m and from 1.7 to 2.9 m respectively. Ice ridge porosity varied within the interval of 7-16 %, while the porosity of non-consolidated part of keel was within the interval of 7-21 %. The mean thickness of consolidated layer of ice ridges varied from 2.4 to 3 m. One ice ridge is observed as an example of an influence of secondary ridging processes on the consolidated layer boundaries and thickness. Comparison of the structure of real ice ridge and the result of computational modeling and laboratory simulation shows the good fit with laboratory ice ridge.

INTRODUCTION

In 2010 Arctic and Antarctic Research Institute (AARI) continues studying the morphometric characteristics of ice ridges in the central part of Arctic basin. Electric thermal drilling of ice ridges with penetration rate recording on a computer, measurement of thickness of ice blocks making up the above-water part of the investigated ice ridges as well as measurements of snow cover height on ridged ice were performed at Barneo ice camp.

Investigation of the structure of ice ridges was carried out by means of electric thermal drilling device of AARI comprising electric thermodrill ETI-3M2 and equipment for penetration rate recording on a laptop. Boreholes were drilled at constant thermal capacity. In addition, the distance from snow (ice) surface to the sea level is measured. The drilling rate depends on the power supply, ice porosity and ice temperature. The thermal drilling data processing gives such characteristics as the above-water and under-water parts of the ice cover, the boundaries of the consolidated layer (CL) of the ice ridge, the boundaries of the voids and the boundaries of ice layers of various porosities. This technology is protected by patent of Russia No. 2153070 (Morev et al., 2000).

Schemes, detailed descriptions of the thermal drilling methods and examples of recording the penetration rate of ice ridge drilling can be seen in the papers (Morev et al., 2000; Kharitonov, 2005(I and II)). One or two lines were passed on each ice ridge intersecting its crest at right angles. Points were marked along the lines at which drilling was conducted with penetration rate recording. Snow cover height at the drilling site was determined from the penetration rate record; and in some cases, by snow survey stakes. Measurement of distance from the snow

(ice) cover surface to the sea level by a special water-level gauge in the well under low freezing temperatures was ineffective because the tip of the meter quickly froze around at contact with sea water. Since in the well drilled to the end water is set at the sea level and after removing the thermodrill begins to freeze, distance from the snow (ice) cover surface to the sea level was measured by a tape measure after well freezing.

RESULTS

During operation of the ice camp (1.04.10–26.04.10) it is impossible to study ridged formations over a large area. Four ice ridges with different morphology near the camp were selected for the work. The main morphometric characteristics of the ridges under consideration are demonstrated in Table 1. Figure 1 shows photos of the ridges.

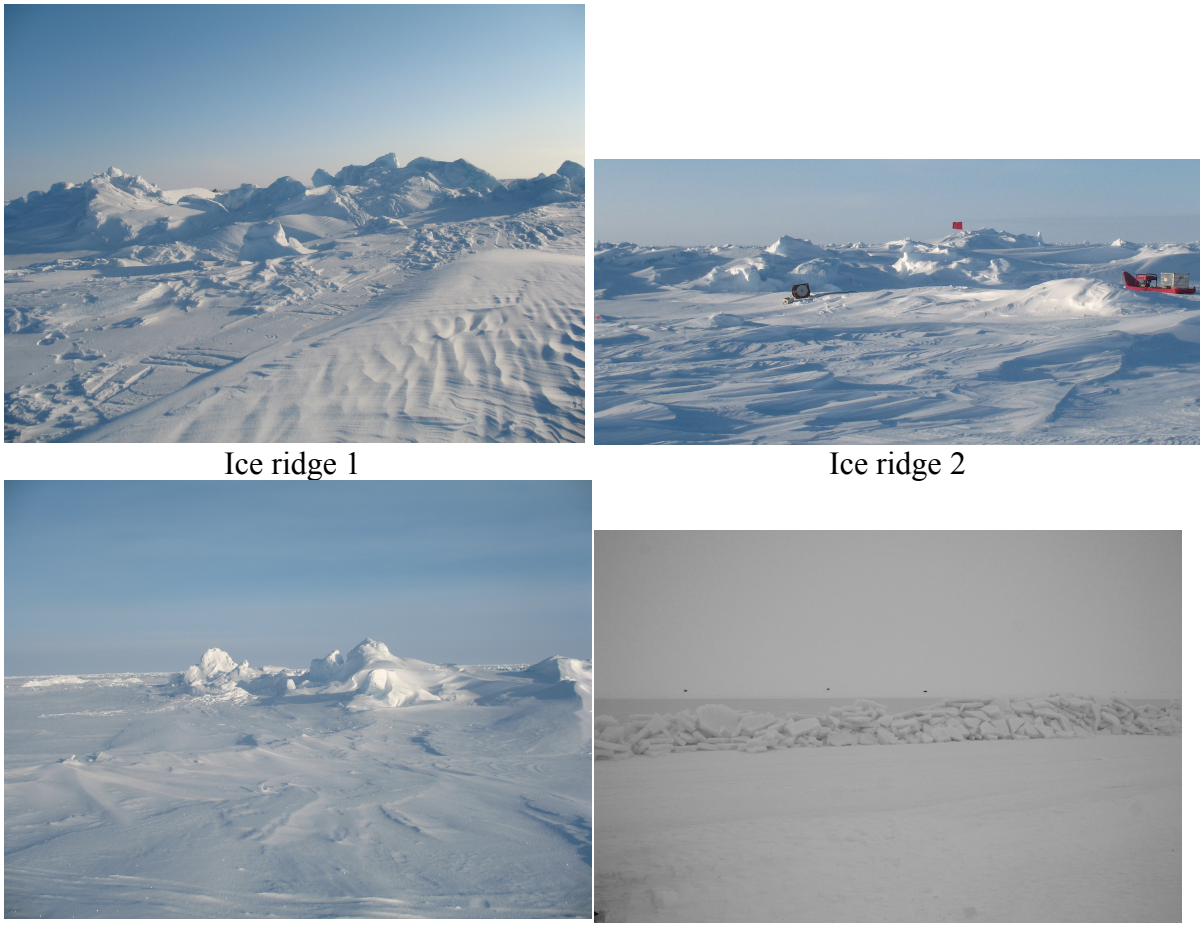

Ice ridge 1 Ice ridge 2

Ice ridge 3 Ice ridge 4

Figure 1. Photos of the ridges under consideration

The first of the studied ice formations represented one of several ice ridges located in close proximity to each other and forming a field of ridged ice. This ridged formation was the largest among those investigated during seasonal works in 2010. Keel width of this ice ridge along the drilling profile was 64 m; maximum total ice thickness was 13.4 m. Fig. 2 shows two drilling profiles of ice ridge 1.

The second of the studied ridged formations was represented by small ridge formed at the end of the ice field opposite to the first ice ridge. Keel width of ice ridge 2 along the drilling profile was about 60 m; maximum total ice thickness was 9.5 m. Profile (cross section) of ice ridge 2 is shown in Fig. 3(a). From drilling results it can be concluded that this ridged formation is a secondary ice ridge. The left part of the drilling profile to point 7 corresponds

to the primary ice ridge as indicated by the average thickness of blocks in this part of the sail – 0.26 m and a greater thickness of the CL. The right part of the profile corresponds to the result of secondary ice ridge formation, when younger ice started ridging onto a rather consolidated primary ice ridge. This is confirmed by the average thickness of crest blocks (between drilling points 7 and 9) – 0.18 m and a relatively small CL thickness in this part of the ridged formation. Total porosity of the left side of ice ridge 2 between drilling points 3 and 7 is 0.03, keel porosity is 0.01. Total porosity of the right side of ice ridge 2 between drilling points 8 and 13 is 0.10, keel porosity is 0.09. It seems that primary ice ridge is second-year ice ridge.

Table 1. Basic characteristics of investigated ice ridges near Barneo ice camp (by records of electrical thermal drilling in 2010).

	Ice ridge			
	1	**2**	**3**	**4**[1]
Number of boreholes	14, 17[2]	15	13	25
Maximum total ice thickness [m]	13.39	9.54	9.00	3.68
Average total ice thickness [m]	8.36	7.70	5.79	2.28
Maximum sail height [m]	2.86	2.61	1.73	1.88
Average sail height [m]	0.87	0.59	0.88	0.76
Maximum keel depth [m]	11.95	8.69	7.27	-
Average keel depth [m]	7.49	5.74	4.90	-
Average ice block thickness / standard deviation [m]	0.60/0.30	0.26/0.08 0.18/0.04[3]	0.41/0.22	0.13/0
Average CL thickness [m]	2.36	3.02	2.67	0.44[4]
Maximum level ice thickness nearby ice ridge [m]	2.49	2.17	2.86	1.70
Minimum level ice thickness nearby ice ridge [m]	1.36	1.66	0.89	0.31
Average level ice thickness nearby ice ridge [m]	1.72	1.90	1.78	-
Sail slope angle [degree]	13.1-24.5	20.5-21.0	18.3-23.5	32.4-36.9
Keel slope angle [degree]	15.9-57.8	15.8-18.1	30.3-40.7	-
Average sail porosity	0.10	0.20	0.14	0.23
Average porosity of nonconsolidated part of keel	0.21	0.09	0.07	-
Average total porosity	0.16	0.09	0.07	-
Ratio of the maximum keel to maximum sail	4.2, 5.0[2]	3.3	4.2	-
Ratio of the average CL thickness to average total ice thickness	0.28	0.39	0.46	-
Ratio of the average CL thickness to average level ice thickness nearby ice ridge	1.37	1.59	1.50	1.32[4]
Maximum snow thickness on the ice ridge [m]	1.74	1.40	1.22	0.27
Minimum snow thickness on the ice ridge [m]	0	0	0.02	0
Average snow thickness on the ice ridge [m]	0.56	0.60	0.36	0.03

[1] Keel of ice ridge 4 was absent.

[2] On 1 and 2 lines.

[3] Upper values for the left part of ice ridge (to point 3, see Fig. 3a) and lower ones for the right part (since point 5).

[4] CL makes sense only on the right side of the ice ridge 4 where the blocks of thin ice are consolidated.

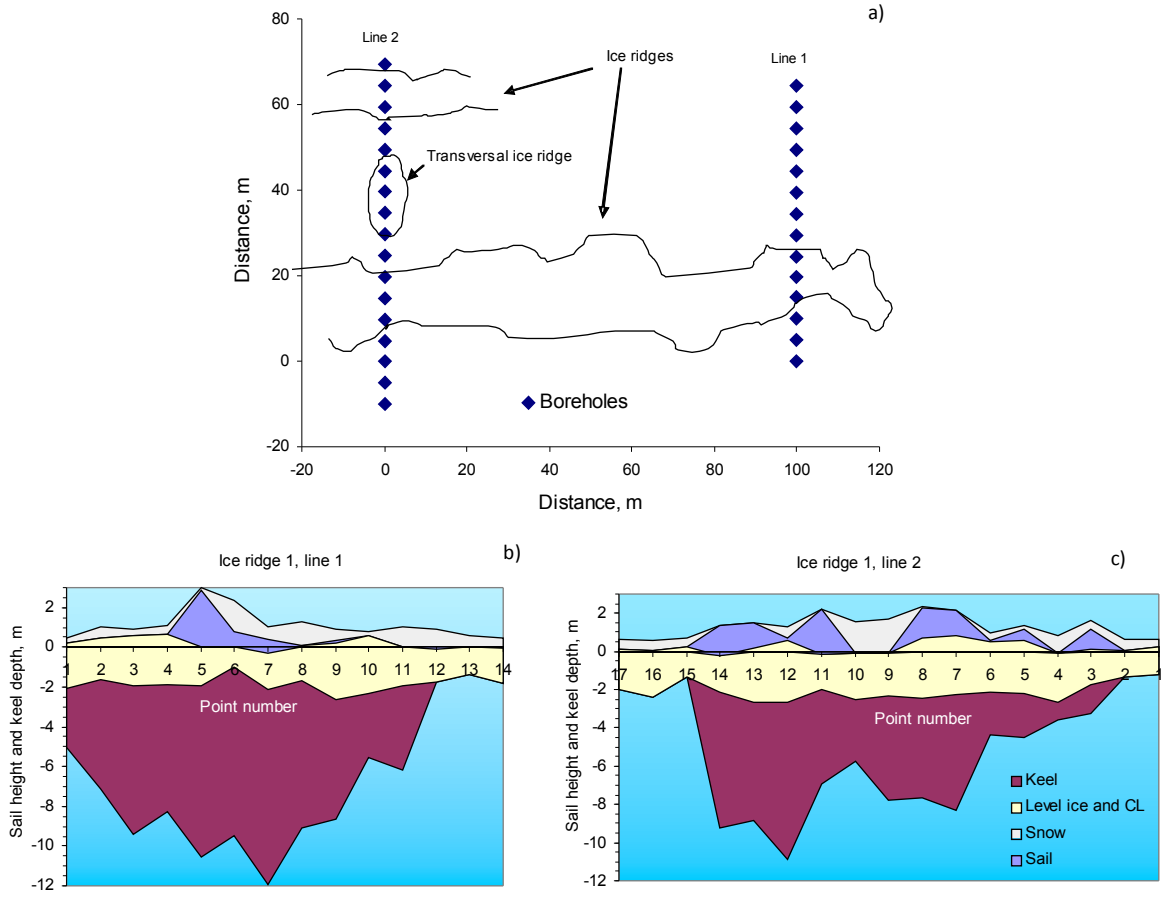

a – Sketch of ice ridge 1; b, c – Cross-sectional profiles of thermodrilling on ice ridge 1. Distance between the points was about 5 m; c – Ice ridge 3. Distance between the points was about 2.5 m; d – Ice ridge 4. Distance between the points was 0.5 m.

Figure 2. Resulting cross-sectional profiles of thermodrilling on ice ridge 1.

Another investigated ice ridge was at the boundary of a multiyear ice field, on which the ice camp was located, and the first-year ice, on which a runway was built. Keel width of this ice ridge along the drilling profile was about 15 m; maximum total ice thickness was 9 m. Profile (cross section) of ice ridge 3 is shown in Fig. 3(b).

Ice ridge 4 formed on 13.04.2010 due to compression of ice of the frozen water lead. Thin ice was driven to the surface of thick ice and formed a ridge sail. Thickness of thin ice was 0.13 m; that of thick ice was on the average 1.63 m. Thickness of thin ice is to thickness of thick ice as 1 is to 12.5 about. After eight days, drilling of the intersecting profile of this ice ridge was performed with 0.5 m spacing between boreholes. Impact of cold on ice ridge 4 was determined by air temperature and evaluated at the time of drilling at 154 degree-days of frost. Keel width of this ice ridge along the drilling profile was about 6 m; maximum total ice thickness was 3.7 m. Drilling profile of ice ridge 4 is shown in Fig. 3(c).

ANALYSIS AND DISCUSSION

The drill penetration rate V is inversely proportional to the volumetric content of the ice solid phase VCI. Thus, dependence of inverse rate (s/m) versus depth is, in fact, the dependence of solid phase volumetric content versus depth, or, in other words, the distribution of solid phase along the borehole expressed in relative units, because the proportionality factor has the dimension of the penetration rate. Every borehole has its own specific distribution. As a result

of drilling, there were 25 linear distributions of volumetric ice content with depth. Next, a grid based on multiple X and Y values is built, where X is an array of values of distance along the profile (linear coordinates of drilling points); and Y, an array of values of depth readings on records. On this grid, *VCI* surface is built; the colour of the surface nodes is assigned by *VCI* values. Dark colour corresponds to voids; white colour, hard ice. Intermediate grey colours correspond to porous ice. Linear colour interpolation between grid nodes is realised. Fig. 4 presents section of ice ridge 4 constructed applying this procedure.

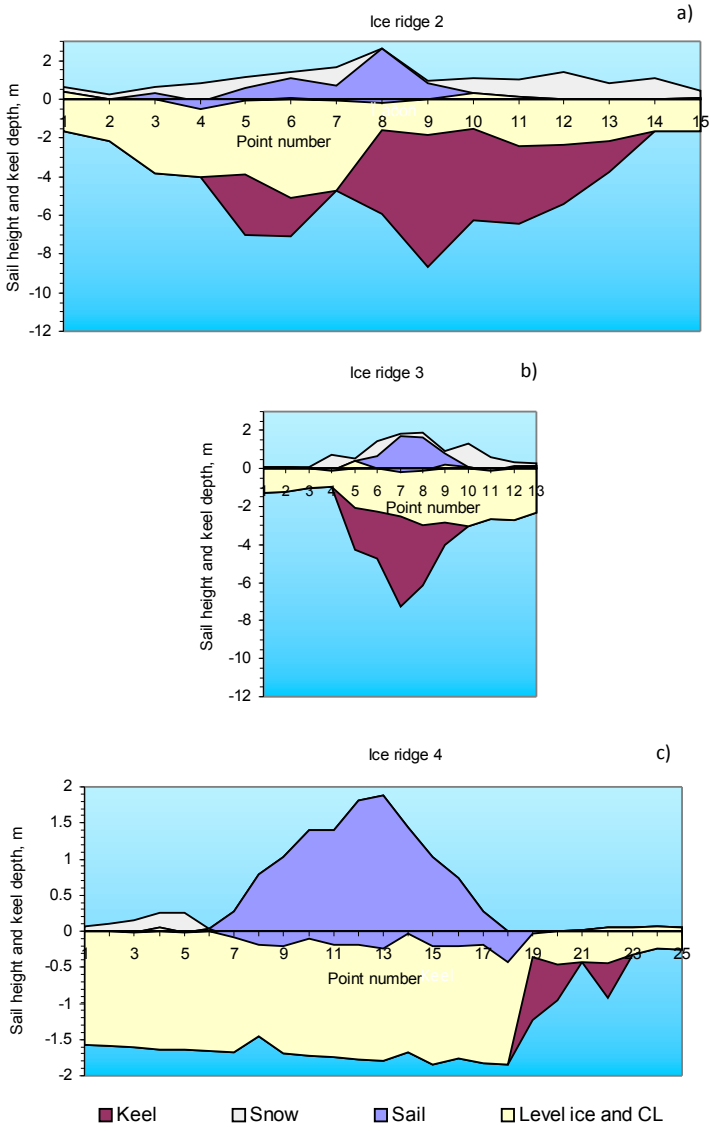

a – Ice ridge 2. Distance between the points was about 5 m; b – Ice ridge 3. Distance between the points was about 2.5 m; c – Ice ridge 4. Distance between the points was 0.5 m

Figure 3. Resulting cross-sectional profiles of thermodrilling on ice ridges 2-4.

Having averaged these distributions for all the holes, it is possible to obtain the average distribution of the volumetric content of the solid phase versus depth for the ice ridge investigated. The CL boundaries determined by this distribution are valid. This procedure of drawing the CL boundaries is described in detail in paper (Kharitonov, 2013).

Fig. 5 shows such distribution for the investigated ice ridges. The CL is distinguished by a marked increase of the volumetric content of solid phase of ice in the area of water level. Due

to a considerable age of ridged formations, especially of ice ridges 2 and 3, the lower boundary of the CL is well pronounced. As mentioned above, the CL of ice ridge 2 is inhomogeneous because of the secondary nature of the ice ridge. In Fig. 5(b) this is confirmed by the fact that the CL of ice ridge 2 seems to be divided into two components. A smaller thickness corresponds to one part of the ice ridge profile; a larger one, to the other part, where the CL is thicker. The distribution of volumetric content of the solid phase of ice of ridge 4 above water level, where it has a much larger spread of values as compared with other ice ridges, corresponds to piling of thin ice fragments. Below water level, this distribution corresponds to a thick ice field, and only a small "tongue" in the depth range of 0...–0.5 m corresponds to the CL formed from thin fragments.

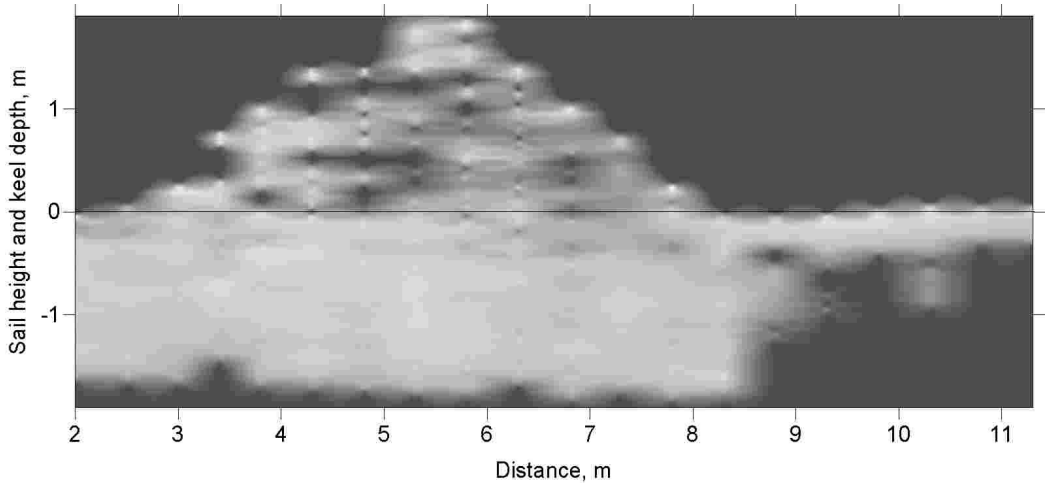

X-axis and Y-axis scales are identical. Horizontal line shows a sea level.

Figure 4. Internal structure of the ice ridge 4 reconstructed of the thermal drill holes.

Porosities of ice ridge 1 and 3 are low compared to what is often given in the literature (see e.g. Høyland, 2002; Leppäranta et al., 1995). In spite of their low porosity the ice ridge 1 and 3 seem to be first-year ice ridges. Author observed two first-year ice ridges at "North Pole – 38" drifting station with the same low porosity (Kharitonov, 2012).

Margin of thick flat ice was submerged under the weight of displaced broken ice of the water lead (Fig. 3(c), points 7-18). Kovaks and Sodhi (1979) give a succession of ridging stages of ice fields in case of a great difference in thickness. They also observed submerging of thick ice under the weight of the displaced broken ice. However, unlike submerging of thick ice from the side of the sail opposite to thin ice observed by Kovacs and Sodhi, in our case submerging of thin ice near the ice ridge sail occurred (Fig. 3(c), point 19). Height of the sail and keel draft of the forming ice ridge observed by Kovacs and Sodhi are approximately the same. Hopkins (1994) numerically simulated the ridging processes of ice fields with a significant difference in thickness. Comparing the results of his simulation and Fig. 3(c) it can be presumed that with such large difference in the thickness of ridging ice numerical calculations do not quite correctly reflect the actual process of ice ridging. According to Hopkins' model, first, a ridge keel forms, and piling of thin ice blocks on thick flat ice is much less pronounced. In our case, almost the entire mass of ridging thin ice was displaced onto the surface of thick ice. Tyshko (2009) conducted field investigations and laboratory modelling of the ridging processes of ice fields with thickness relationship over 3:1. Fig. 6 shows his kinematic scheme of formation of a block ice ridge in the process of thin ice field ride up on a thicker one. If it is presumed that the formation of ice ridge 4 stopped at stage d, when only

the ice ridge sail had formed, its structure agrees well with the ridging scheme given by Tyshko.

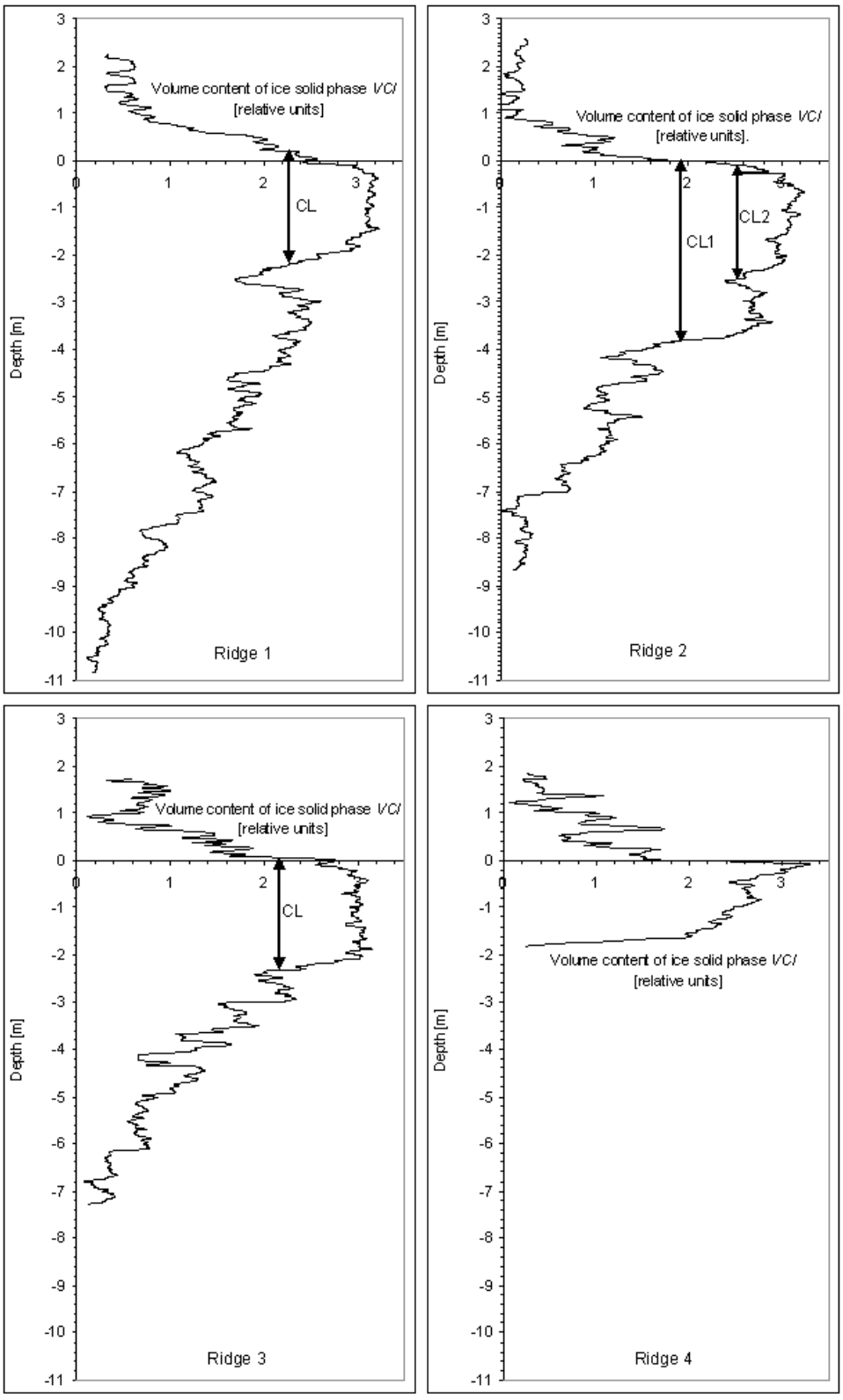

CL1 is mean CL thickness in the left part of ice ridge 2. CL2, mean CL thickness in the right part of ice ridge 2 (see Fig. 3(a)).

Figure 5. Depth-wise distribution of the volume content of ice solid phase (*VCI*) of ice ridges investigated in 2010 at Barneo ice camp (according to the electric thermal drilling data).

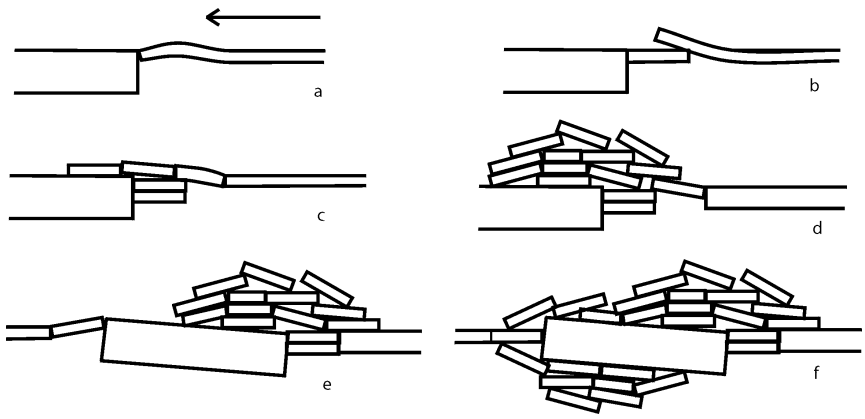

Figure 6. Kinematic scheme of formation of a block ice ridge in the process of thin ice field ride up on a thicker one (Tyshko, 2009).

CONCLUSIONS

It can be concluded that in the spring season of 2010 the choice of objects for the study was successful. All the investigated ridged formations had different morphology. Morphometric characteristics of ice ridges are, as a whole, consistent with the generally accepted notions. CL thickness of first-year ice ridges in the central Arctic Basin is greater than that of the CL of first-year ice ridges in marginal freezing seas. On the example of ice ridge 2, it is clearly seen how the processes of secondary ice ridge formation affect the boundaries and thickness of the CL of the ice ridge. The ratio "average thickness of the CL / average thickness of the ice ridge", which points to the consolidation degree of the ice ridge, was within 0.28-0.46. The ratio "average thickness of the CL / average thickness of flat ice" ranged within 1.32-1.59, which is characteristic of first-year ice ridges. Comparison of the structure of a real ice ridge with results of mathematical and laboratory modeling showed a good agreement with the laboratory ice ridge. However, for the final conclusion about correctness of the mathematical model of Hopkins it is necessary to carry on the studies of the results of ice ridge formation during interaction of ice fields with a significant difference in ice thicknesses.

REFERENCES

Hopkins, M. A., 1994. On the ridging of intact lead ice. – J. Geophys. Res., Vol. 99, C8, pp. 16351-16360.

Høyland, K. V., 2002. Consolidation of first-year sea ice ridges. Journal of Geophysical Research 107 (C6, 10.1029/2000JC000526), 15,1-15,15.

Kharitonov, V. V., 2005. Experimental'nye issledovaniya vnutrennego stroyeniya torosov i stamukh s pomoschyu termobureniya [Experimental research of the internal structure of ice ridges and stamukhas by thermal drilling methods]. Doctoral thesis (physics and mathematics). AARI, St. Petersburg (in Russian).

Kharitonov, V. V., 2005. Peculiarities of Fractional Composition of the Pechora Sea First-Year Ridges. Proc. of the 18th Int. Conference on Port and Ocean Engineering under Arctic Conditions (POAC). Potsdam, New York, 26-30 June 2005, Vol.2, p. 907-916.

Kharitonov, V. V., 2012. Internal structure and porosity of ice ridges investigated at «North Pole 38» drifting station. Cold Regions Science and Technology 82 (2012) pp. 144–152.

Kharitonov, V. V., 2013. Distribution of ice volume content in sea ice ridges. Submitted at POAC'13.

Kovacs, A. and Sodhi, S. D. 1979. Ice pile-up and ride-up on Arctic and subarctic beaches. POAC'79. V.1. pp. 127-146.

Leppäranta, M., Lensu, M., Koslof, P., Veitch, B., 1995. The life story of a first-year sea ice ridge. Cold Regions Science and Technology (23), 279-290.

Morev, V. A., Morev, A. V., Kharitonov, V. V., 2000. Sposob opredeleniya struktury torosov i stamukh, svoistv l'da i granitsy l'da i grunta [Method of determination of ice ridge and stamukha structure, ice features and boundaries of ice and ground]. Patent of Russia №2153070, Bulletin of inventions, 20 (in Russian).

Tyshko, K. P., 2009. Formation and consolidation of hummocks on the Arctic sea's one-year ice cover as a result of laboratory and field researchers. Russian Meteorology and Hydrology (ISSN 1068-3739, Vol. 34, No. 8), pp. 534-540.